Scambler P, Morrow B, Driscol DA, Moons L, Esguerra CV, Carmeliet G, Behn-Krappa A, Devriendt K, Collen D, Conway SJ, Carmeliet P (2003) VEGF: a modifier of the del22q11 (DiGeorge) syndrome? *Nat Med* **9:** 173–182

Takashima S, Kitakaze M, Asakura M, Asanuma H, Sanada S, Tashiro F, Niwa H, Miyazaki Ji J, Hirota S, Kitamura Y, Kitsukawa T, Fujisawa H, Klagsbrun M, Hori M (2002) Targeting of both mouse neuropilin-1 and neuropilin-2 genes severely impairs developmental yolk sac and embryonic angiogenesis. *Proc Natl Acad Sci USA* **99:** 3657–3662

Veikkola T, Alitalo K (1999) VEGFs, receptors and angiogenesis. *Semin Cancer Biol* **9:** 211–220

West DC, Rees CG, Duchesne L, Patey SJ, Terry CJ, Turnbull JE, Delehedde M, Heegaard CW, Allain F, Vanpouille C, Ron D, Fernig DG (2005) Interactions of multiple heparin binding growth factors with neuropilin-1 and potentiation of the activity of fibroblast growth factor-2. *J Biol Chem* **280:** 13457–13464

Zachary I (2001) Signaling mechanisms mediating vascular protective actions of vascular endothelial growth factor. *Am J Physiol Cell Physiol* **280:** C1375–C1386

Basic Res Cardiol 101:465–470 (2006)
DOI 10.1007/s00395-006-0603-6

Hideaki Kanzaki
Satoshi Nakatani
Naoaki Yamada
Shin-ichi Urayama
Kunio Miyatake
Masafumi Kitakaze

Impaired systolic torsion in dilated cardiomyopathy: Reversal of apical rotation at mid-systole characterized with magnetic resonance tagging method

Received: 2 November 2005
Returned for revision: 22 November 2005
Revision received: 20 April 2006
Accepted: 11 May 2006
Published online: 16 June 2006

Presented in part at the Annual Scientific Session of ACC 2004 in New Orleans, USA
There are no financial obligations that could lead to conflict of interest regarding this study.

H. Kanzaki, MD · S. Nakatani, MD · K. Miyatake, MD · M. Kitakaze, MD
Department of Cardiology
National Cardiovascular Center
Osaka, Japan

S. Nakatani, MD (✉)
Department of Cardiology
National Cardiovascular Center
5-7-1, Fujishiro-dai, Suita
Osaka 565-8565, Japan
Tel.: +81-6/6833-5012
Fax: +81-6/6872-7486
E-Mail: nakatas@hsp.ncvc.go.jp

N. Yamada, MD
Department of Radiology
National Cardiovascular Center
Osaka, Japan

S.-I. Urayama, PhD
Department of Investigative Radiology
National Cardiovascular Center Research Institute
Osaka, Japan

Abstract Left ventricular (LV) torsion plays an important role in squeezing the blood out of the heart. To characterize the systolic torsion in LV dysfunction, we studied using magnetic resonance imaging myocardial tagging method in 26 subjects: 17 patients with dilated cardiomyopathy (DCM, LV ejection fraction [EF], 27 ± 8 %) and 9 healthy control subjects. Grid-tagged LV short-axis cine images were acquired at base, mid and apex levels. Tag-intersections were tracked during the systole, thereby determining rotation angle (positive indicated clockwise from the apex). Peak torsion was defined as the maximum difference in rotation angle between the base and apex. Time to peak torsion was expressed as % systole by dividing the time by a total systolic time. Amplitude of the rotation at peak was less in DCM than in controls at both the base (0.1 ± 2.9 vs. 2.6 ± 1.6°, $P < 0.05$) and apex (−5.9 ± 5.3 vs. −11.2 ± 2.5°, $P < 0.01$). Amplitude of peak torsion was then less in DCM than in controls (6.1 ± 3.4 vs. 13.6 ± 2.5°, $P < 0.001$), and the timing of peak was earlier (66 ± 22 vs. 104 ± 16 % systole, $P < 0.001$). The amplitude of peak torsion was correlated with LVEF ($r = 0.74$, $P < 0.001$). In conclusion, amplitude of systolic torsion was impaired in proportion to LV function. Systolic torsion in LV dysfunction was characterized by the discontinuing counter-rotation of the apex to the base before end-systole.

Key words magnetic resonance imaging – cardiomyopathy – heart failure – torsion

Abbreviations and Acronyms DCM: dilated cardiomyopathy; ECG: electrocardiogram; LV: left ventricular; LVEDP: LV end-diastolic pressure; LVEDV: LV end-diastolic volume; LVEF: LV ejection fraction; LVESV: LV end-systolic volume; MR: magnetic resonance; NYHA: New York Heart Association; SPAMM: spatial modulation of magnetization

Introduction

The myocardial fibers of the left ventricle vary in orientation across the wall [13, 22, 25]. Greenbaum et al. [13] reported the changes in orientation of the myocardial fibers from a right hand helix in the subendocardium as viewed from the apex, through circumferential fibers in the midwall, to a left hand helix in the subepicardium. Torrent-Guasp et al. [25, 26] have shown that the myocardial fibers constitute a continuous muscular band. The band is oriented spatially as a helix formed by basal and apical loops. Buckberg et al. [4–6] have suggested that the spiral form of myocardial fibers results from twist of the primitive heart evolving from a singular tube. Coghlan et al. [7] proposed that the myocardial

fiber orientation also affects the sequence of activation because of the anisotropic left ventricular (LV) conduction.

During systole, the LV apex rotates in a counterclockwise direction relative to the LV base which rotates in a clockwise direction about LV long-axis as viewed from the apex [30]. This wringing motion is relevant to the shortening of these obliquely oriented LV fibers [21]. Several studies have suggested that LV torsion was sensitive to changes in contractility, but essentially unaffected by changes in pressure or volume loading [3, 15, 17]. However, details of cardiac torsion in patients with impaired LV function still remain unclear.

Several modalities have been used to describe and quantify cardiac torsion, including the magnetic resonance (MR) tagging method with spatial modulation of magnetization (SPAMM). This method makes it possible to label the myocardium non-invasively with spatially selective radiofrequency pulses [1]. Deformation of the tagged pattern reflects the motion of the underlying myocardium to allow tracking the rotation of a LV short-axis plane [2, 19, 29]. Our objective was to characterize LV torsional deformation in patients with impaired LV function using the myocardial MR tagging method.

Methods

Subjects

The study population consisted of a total of 26 subjects. Seventeen patients (15 males, 2 females, age 43 ± 13 years) diagnosed with non-ischemic dilated cardiomyopathy (DCM) from cardiac catheterization were enrolled (Table 1). There was no subject with left bundle branch block (LBBB) on electrocardiogram (ECG). Both LV volumes and EF were measured from left ventriculogram.

Table 1 Characteristics of 17 patients with dilated cardiomyopathy

NYHA functional class, *n* (%)	
I	13 (76)
III	3 (18)
IV	1 (6)
LVEDV, ml	145±65
LVESV, ml	110±65
LVEF, %	27±8
LVEDP, mmHg	12±5
Cardiac index, L/min/m^2	3.4±0.8
Heart rate, beats/min	73±15
QRS duration, ms	105±12

Data are expressed number (%) or mean ± SD
DCM dilated cardiomyopathy; *NYHA* New York Heart Association, *LVEDV* LV end-diastolic volume; *LVESV* LV end-systolic volume; *LVEF* LV ejection fraction; *LVEDP* LV end-diastolic pressure

The diagnosis of DCM was made from the definitions of the World Health Organization. Nine healthy volunteers performed only MR imaging as controls (9 males, age 34 ± 6 years). All provided written informed consent. The study was approved by the ethics committee and performed according to institutional ethics guidelines.

MR image acquisition

MR imaging was performed on a Magnetom Vision 1.5T system (Siemens Medical Solutions, Erlangen, Germany). First of all, the LV long-axis view was obtained to determine three short-axis planes: the basal (chordae tendineae), mid (papillary muscles), and apical planes (Fig. 1). Secondly as shown in Fig. 2, grids with 8-mm spacing were impressed on the myocardium in the LV short-axis view using the spatial modulation of magnetization (SPAMM) method after the R-wave from ECG. The MR tagged cine images were acquired with a breath-hold segmented k-space sequence. Imaging parameters were as follows: image reconstruction interval, 35 ms; 7 segments echo time, 4 ms; flip angle, 20°; the field of view, 350 × 350 mm; image matrix size, 256 × 256 pixels; slice thickness, 8 mm.

MR image analysis

The MR images were analyzed off-line on a workstation (Indigo2, Silicon Graphics Inc, Mountain View, CA) with the dedicated software as previously described [27]. In brief, throughout a series of the images, this software can identify and track the grid pattern with distribution of tag intersections to superimpose a meshwork consisting of nodes connected with straight lines (Fig. 2). The nodes within the LV cavity and outside the LV myocardium were removed manually. First of all, the mesh-

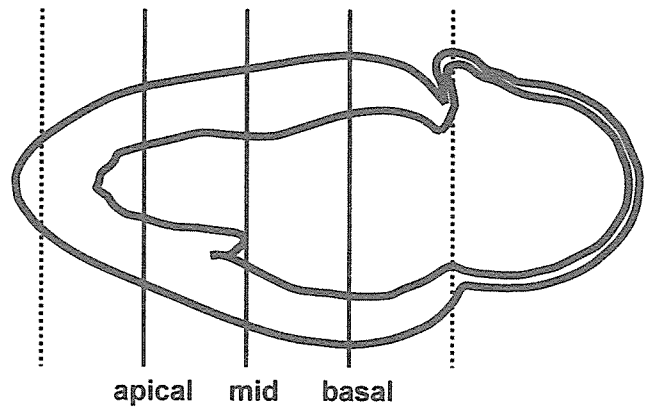

Fig. 1 By dividing equally long-axis of the left ventricle into four compartments, MR tagged short-axis images were acquired at the three levels: chordae tendineae (base), papillary muscles (mid), and apical planes (apex)

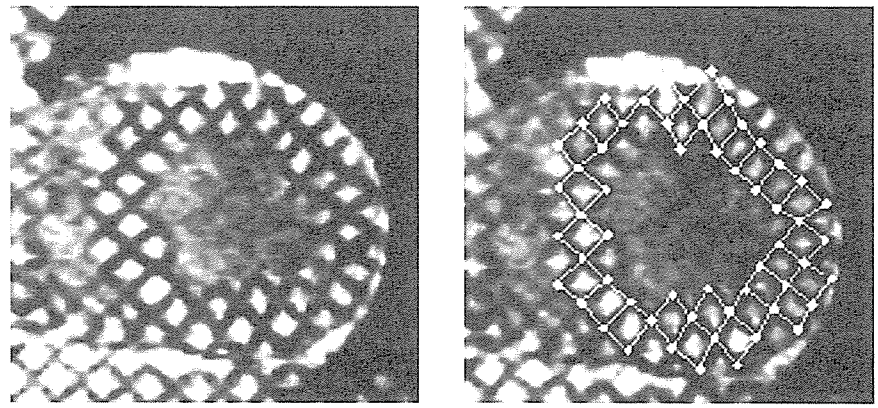

Fig. 2 An acquired image of the mid left ventricular short-axis at end-systole with MR tagging method (Left). A meshwork superimposed on the grid-tag pattern (Right)

work was deformed semi-automatically and then re-formed manually at each image. Finally, the software provided all coordinates of the nodes during systole [27].

Displacement of each node from an initial position was determined during systole as angular displacement relative to the moving centroid at each frame. Rotation angle of each LV short-axis plane was given by averaging measurements from angular displacement of all intersections on the myocardium. LV torsion was defined as the difference in rotation angle between the basal and apical planes (Fig. 3). The gradient of LV torsion was calculated by dividing magnitude of the LV torsion by the distance between the basal and apical planes. Positive degrees indicated a clockwise rotation as viewed from the apex.

We defined the time to peak rotation in % systole as the time from R-wave of ECG to the maximum rotational displacement divided by a total systolic time. LV short-axis diameter was obtained from the inner tag-intersections on the myocardium at the mid LV plane. The total systolic time was measured as the interval from the R-wave to the moment of minimum short-axis diameter of the left ventricle.

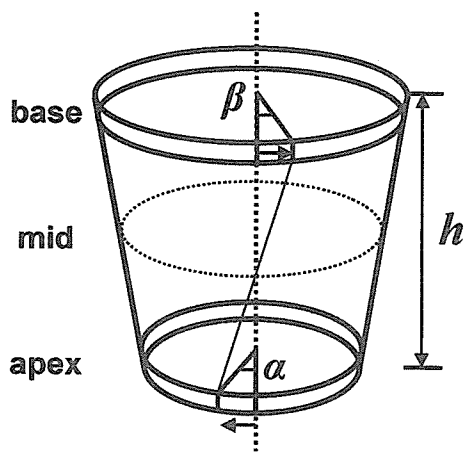

Fig. 3 LV torsion was defined as the difference in rotational angles of basal (β) and apical (α) planes. Torsional gradient was calculated by dividing the LV torsional angle by the distance between the two planes (*h*)

Statistics

Results are expressed as mean values ± SD. Continuous variables were compared with one-way ANOVA. Linear regression analysis was used to assess the relationship between two groups. All statistical tests were performed with StatView 5.0 for Windows (SAS Institute, Cary, USA). Statistical significance was assumed for $P < 0.05$.

Results

Cardiac torsion

In controls (Fig. 4a), both the LV base and apex initially rotated counterclockwise. After 21 ± 6 % systole, the base changed the direction of rotation to clockwise, whereas the apex maintained counter-clockwise rotation until around the end-systole. Peak cardiac torsion of 13.6 ± 2.5° was generated at 104 ± 10 % systole. In other words, the peak of torsion almost coincided with end-systole.

In patients with DCM (Fig. 4b), both base and apex initially rotated counter-clockwise as well. However, the base changed the direction somewhat late (at 27 ± 8 % systole, $P < 0.05$ vs. control), and the apex also followed to turn toward clockwise at mid-systole (at 54 ± 18 % systole, $P < 0.05$ vs. control). Then cardiac torsion peaked at 66 ± 8 % systole in patients with DCM (about 12 % systole behind the apical peak), which was earlier than in controls ($P < 0.001$). The magnitude of torsion in patients with DCM was also markedly impaired (6.1 ± 3.4°, $P < 0.0001$ vs. control).

As shown in Fig. 5, the peak apical rotation in controls was −11.2 ± 2.5° and the basal rotation was 2.6 ± 1.6°, thereby developing the peak LV torsional gra-

Basic Research in Cardiology, Vol. 101, No. 6 (2006)

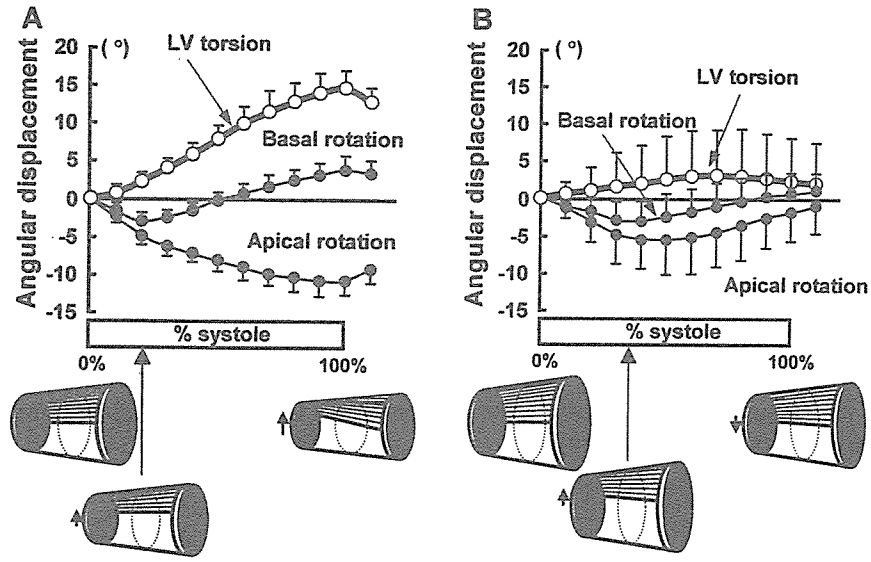

Fig. 4 Time course of LV torsion in controls (**a**) and DCM (**b**): Instantaneous LV torsion (○) was developed from the net difference between the basal and apical rotations (●). Positive degrees indicate a clockwise rotation as viewed from the apex

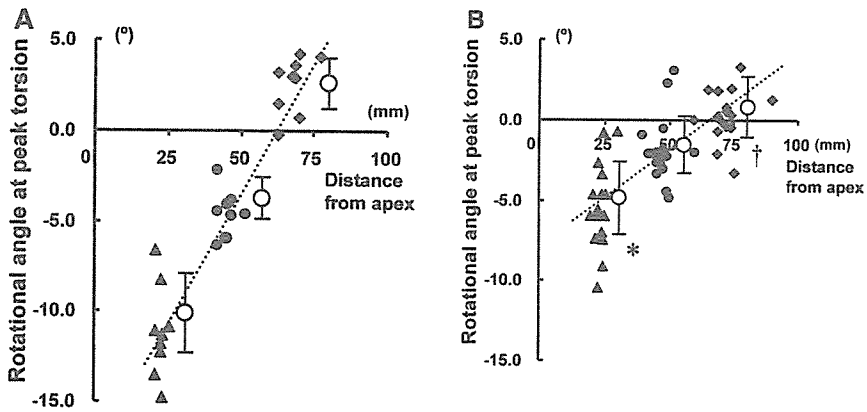

Fig. 5 The rotational angles (of ▲ apical, ● mid, and ◆ basal planes) and the distance from the LV apex at the peak torsion in controls (**a**) and DCM (**b**). The broken line represents the mean of the individual torsional gradients, which was significantly less in DCM than controls. * $P < 0.01$ and ** $P < 0.05$ vs. control. Positive degrees indicate a clockwise rotation as viewed from the apex

dient of 3.0 ± 0.5°/cm. In patients with DCM, the rotation was impaired at the both apical (-5.9 ± 5.3°, $P < 0.01$ vs. control) and basal levels (0.1 ± 2.9°, $P < 0.05$ vs. control). Consequently, the peak LV torsional gradient was markedly impaired (1.3 ± 0.8°/cm, $P < 0.01$ vs. control).

Cardiac torsion and LV function

The magnitude of peak torsion and torsional gradient showed significant correlations with LVEF ($r = 0.74$ and $r = 0.78$, respectively, both $P < 0.001$) as shown in Fig. 6. Time to the peak LV torsion was correlated with the LV end-diastolic volume ($r = -0.71$, $P < 0.005$), end-systolic volume ($r = -0.80$, $P < 0.001$), and magnitude of peak torsion ($r = 0.81$, $P < 0.0001$).

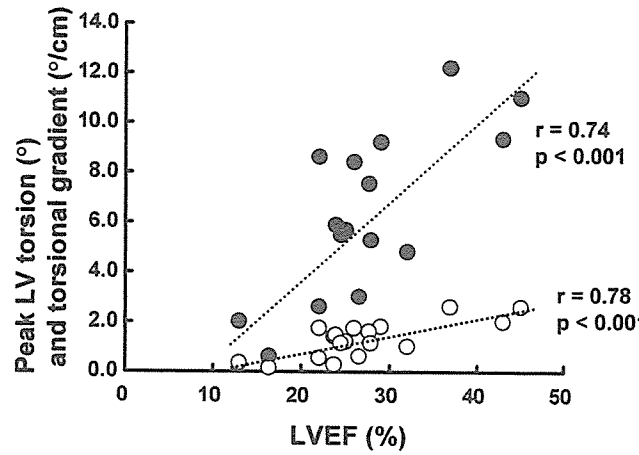

Fig. 6 Peak LV torsional angle (●) and torsional gradient (○) were correlated well with LVEF in patients with DCM

Discussion

The present study revealed that phasic analysis of both apical and basal rotations need to obtain the cardiac torsion of the failing heart. In DCM hearts, at both the basal and apical planes, the amplitude of peak rotation was significantly less than those in normal hearts. The timing of peak torsion did not coincide with the timing of peak apical rotation and the end-systole.

Impaired cardiac torsion in LV dysfunction

The normal control data in Fig. 5 are consistent with the data reported by the group of Hess [18]. The magnitude of peak LV torsion has been reported to be 11–19°, and torsional gradient was 2.8–3.4°/cm in normal humans [2, 14–18, 23, 29]. The present results, $13.6 \pm 2.5°$ and $3.0 \pm 0.5°$/cm, respectively, in controls are consistent with the previous reports, supporting the validity of the present method.

In contrast, the magnitude of peak torsion and torsional gradient in DCM remarkably decreased to $6.1 \pm 3.4°$ and $1.3 \pm 0.8°$/cm, respectively. The peak of torsion was at neither end-systole nor the timing of peak apical rotation, approximately 12% systole behind the apical peak (Fig. 4b). Taber et al. [24] proposed that LV contractility and cavity volume can influence the torsion using theoretical models. LV torsion is due to the decreasing ventricular radius and increasing wall thickness, which further increase the mechanical advantage of the outer layers. In markedly dilated heart, the advantage over the inner layers is lost.

Sallin et al. [22] demonstrated the rationale that the spiral configuration enabled the myocardial fibers with only 15% shortening to generate LVEF up to >60%. Buckberg et al. [5] proposed that flattening of the apical loop architecture in the spheric DCM heart cause reduced LVEF. LV dilatation can make the apical loop become more basal through more transverse fiber orientation.

Significance of LV torsion

Many investigators have focused on cardiac torsion as a sensitive marker of global LV function [12, 14–16, 18–20]. Nagel et al. [18], using the similar grid technique, reported that systolic torsion was correlated with percentage change in LV area determined as regional EF. Dong et al. [8] reported that torsion was correlated with stroke volume and LVEF in animal experiments. We showed the good correlation between the rotational amplitude and LVEF in humans as well (Fig. 6). Rademakers et al. [20] proposed that torsion recoil in diastole could aid LV filling with sucking in blood from the left atrium. Rothfeld et al. [21] demonstrated that LV systolic torsion related with acceleration and acceleration time of mitral early-diastolic filling wave from echocardiography. In other words, cardiac torsion is a possible mechanism by which potential energy can be stored in systole and then released in early diastole to create LV suction [28]. A tight coupling has been reported between contraction and relaxation [9]. Our results showing that cardiac torsion was associated with systolic function may support the idea that cardiac torsion plays a role of a flywheel or pendulum.

Clinical implications

Cardiac resynchronization therapy using a biventricular pacing system is effective for synchronization of wall motion in heart failure patients with LBBB. Recognition of the influences of LBBB on rotation and time-to-peak rotation may help improved understanding of the electrical activation sequence in obliquely oriented myocardial fibers. Fonseca et al. [11] reported that the three dimensional MR tissue tagging technique was useful for analysis on asynchrony and torsion. Recent development of tissue tracking technique of ultrasound also allows easy assessment of torsion in patients with LBBB. Further work in this area is expected.

Study limitations

There are some limitations in the present study. First, use of the tag spacing of 8 mm on the LV myocardium with wall thickness of < 11 mm can lead heterogeneous distribution of the intersecting points [27]. We averaged all values measured from intramyocardial grid-crossing points to assess a rotation of the plane. Reproducibility was not examined. Second, the systolic through-plane motion of short-axis images can cause some error. However, because this motion is remarkable at the base of the left ventricle which shows further less rotation than the apex, the error may not be critical for the present results. Fischer et al. [10] have resolved this problem by tracking the tags on the same slice of the myocardium. Third, frame rate is approximately 30 fps in the MR imaging method. This may be slightly low in measuring the peak value of LV torsion and time to peak torsion. Fourth, the mean age of our control group is less than that of the DCM group. This could be a limitation because of the effect of age. Fifth, no MR imaging data on LV volume was available in the present study. Therefore, we had to use the volume data from left ventriculogram instead of that.

Conclusion

The apex and base rotated with an opposite direction to generate effective torsion at end-systole in normal hearts. In DCM hearts, amplitude of peak LV systolic torsion was impaired in proportion to the global LV function. Systolic torsion in LV dysfunction was characterized by the discontinuing counter-rotation of the apex to the base before end-systole as it might follow the basal motion.

Acknowledgement The authors gratefully acknowledge Mr. Jason Catizone for the preparation of this manuscript and Toshiharu Sakuma, BS RT for the technical assistance.

References

1. Axel L, Dougherty L (1989) MR imaging of motion with spatial modulation of magnetization. Radiology 171:841–845
2. Buchalter MB, Weiss JL, Rogers WJ, Zerhouni EA, Weisfeldt ML, Beyar R, Shapiro EP (1990) Noninvasive quantification of left ventricular rotational deformation in normal humans using magnetic resonance imaging myocardial tagging. Circulation 81:1236–1244
3. Buchalter MB, Rademakers FE, Weiss JL, Rogers WJ, Weisfeldt ML, Shapiro EP (1994) Rotational deformation of the canine left ventricle measured by magnetic resonance tagging: effects of catecholamines, ischaemia, and pacing. Cardiovasc Res 28:629–635
4. Buckberg GD (2001) The structure and function of the helical heart and its buttress wrapping. II. Interface between unfolded myocardial band and evolution of primitive heart. Semin Thorac Cardiovasc Surg 13:320–332
5. Buckberg GD, Coghlan HC, Torrent-Guasp F (2001) The structure and function of the helical heart and its buttress wrapping. VI. Geometric concepts of heart failure and use for structural correction. Semin Thorac Cardiovasc Surg 13:386–401
6. Buckberg GD (2002) Basic science review: the helix and the heart. J Thorac Cardiovasc Surg 124:863–883
7. Coghlan HC, Coghlan AR, Buckberg GD, Gharib M, Cox JL (2001) The structure and function of the helical heart and its buttress wrapping. III. The electric spiral of the heart: The hypothesis of the anisotropic conducting matrix. Semin Thorac Cardiovasc Surg 13: 333–341
8. Dong SJ, Hees PS, Huang WM, Buffer SA Jr, Weiss JL, Shapiro EP (1999) Independent effects of preload, afterload, and contractility on left ventricular torsion. Am J Physiol 277(3 Pt 2):H1053–H1060
9. Eichhorn EJ, Willard JE, Alvarez L, Kim AS, Glamann DB, Risser RC, Grayburn PA (1992) Are contraction and relaxation coupled in patients with and without congestive heart failure? Circulation 85:2132–2139
10. Fischer SE, McKinnon GC, Scheidegger MB, Prins W, Meier D, Boesiger P (1994) True myocardial motion tracking. Magn Reson Med 31:401–413
11. Fonseca CG, Oxenham HC, Cowan BR, Occleshaw CJ, Young AA (2003) Aging alters patterns of regional nonuniformity in LV strain relaxation: a 3-D MR tissue tagging study. Am J Physiol Heart Circ Physiol 285:H621–H630
12. Gibbons Kroeker CA, Tyberg JV, Beyar R (1995) Effects of load manipulations, heart rate, and contractility on left ventricular apical rotation. An experimental study in anesthetized dogs. Circulation 92:130–141
13. Greenbaum RA, Ho SY, Gibson DG, Becker AE, Anderson RH (1981) Left ventricular fibre architecture in man. Br Heart J 45:248–263
14. Hansen DE, Daughters GT 2nd, Alderman EL, Ingels NB Jr, Miller DC (1988) Torsional deformation of the left ventricular midwall in human hearts with intramyocardial markers: regional heterogeneity and sensitivity to the inotropic effects of abrupt rate changes. Circ Res 62:941–952
15. Hansen DE, Daughters GT 2nd, Alderman EL, Ingels NB, Stinson EB, Miller DC (1991) Effect of volume loading, pressure loading, and inotropic stimulation on left ventricular torsion in humans. Circulation 83:1315–1326
16. Ingels NB Jr, Hansen DE, Daughters GT 2nd, Stinson EB, Alderman EL, Miller DC (1989) Relation between longitudinal, circumferential, and oblique shortening and torsional deformation in the left ventricle of the transplanted human heart. Circ Res 64:915–927
17. Moon MR, Ingels NB Jr, Daughters GT 2nd, Stinson EB, Hansen DE, Miller DC (1994) Alterations in left ventricular twist mechanics with inotropic stimulation and volume loading in human subjects. Circulation 89:142–150
18. Nagel E, Stuber M, Lakatos M, Scheidegger MB, Boesiger P, Hess OM (2000) Cardiac rotation and relaxation after anterolateral myocardial infarction. Coron Artery Dis 11:261–267
19. Nakatani S, White RD, Powell KA, Lever HM, Thomas JD (1996) Dynamic magnetic resonance imaging assessment of the effect of ventricular wall curvature on regional function in hypertrophic cardiomyopathy. Am J Cardiol 77: 618–622
20. Rademakers FE, Buchalter MB, Rogers WJ, Zerhouni EA, Weisfeldt ML, Weiss JL, Shapiro EP (1992) Dissociation between left ventricular untwisting and filling. Accentuation by catecholamines. Circulation 85:1572–1581
21. Rothfeld JM, LeWinter MM, Tischler MD (1998) Left ventricular systolic torsion and early diastolic filling by echocardiography in normal humans. Am J Cardiol 81:1465–1469
22. Sallin EA (1969) Fiber orientation and ejection fraction in the human left ventricle. Biophys J 9:954–964
23. Stuber M, Scheidegger MB, Fischer SE, Nagel E, Steinemann F, Hess OM, Boesiger P (1999) Alterations in the local myocardial motion pattern in patients suffering from pressure overload due to aortic stenosis. Circulation 100:361–368
24. Taber LA, Yang M, Podszus WW (1996) Mechanics of ventricular torsion. J Biomech 29:745–752
25. Torrent-Guasp F, Ballester M, Buckberg GD, Carreras F, Flotats A, Carrio I, Ferreira A, Samuels LE, Narula J (2001) Spatial orientation of the ventricular muscle band: physiologic contribution and surgical implications. J Thorac Cardiovasc Surg 122:389–392
26. Torrent-Guasp F, Kocica MJ, Corno AF, Komeda M, Carreras-Costa F, Flotats A, Cosin-Aguillar J, Wen H (2005) Towards new understanding of the heart structure and function. Eur J Cardiothorac Surg 27:191–201
27. Urayama S, Matsuda T, Sugimoto N, Mizuta S, Yamada N, Uyama C (2000) Detailed motion analysis of the left ventricular myocardium using an MR tagging method with a dense grid. Magn Reson Med 44:73–82
28. Waldman LK, Nosan D, Villarreal F, Covell JW (1988) Relation between transmural deformation and local myofiber direction in canine left ventricle. Circ Res 63:550–562
29. Young AA, Imai H, Chang CN, Axel L (1994) Two-dimensional left ventricular deformation during systole using magnetic resonance imaging with spatial modulation of magnetization. Circulation 89:740–752
30. Yun KL, Miller DC (1995) Torsional deformation of the left ventricle. J Heart Valve Dis 4(Suppl 2):S214–S220

J Pharmacol Sci **101**, 179 – 181 (2006)

Journal of Pharmacological Sciences

Correspondence

New Therapeutic Application of Erythropoietin Against Ischemic Heart Diseases

Tetsuo Minamino[1] and Masafumi Kitakaze[2,*]

[1]*Cardiovascular Medicine, Osaka University Graduate School of Medicine, Suita, Osaka 565-0871, Japan*
[2]*Cardiovascular Division of Internal Medicine, National Cardiovascular Center, 5-7-1 Fujishirodai, Suita, Osaka 565-8565, Japan*

Received April 25, 2006

Keywords: myocardial infarction, angiogenesis, ventricular remodeling

Erythropoietin (EPO) is a cytokine that promotes proliferation and differentiation of erythroid precursor cells, and it is widely used for the treatment of anemia in patients with chronic renal failure (1). Therefore, EPO has been classified as one of the hemtopoietic cytokines independent of cardiovascular physiological and biochemical actions. However, intriguingly, EPO can also exert anti-apoptotic and radical scavenging effects on non-erythroid cells (1). Furthermore, EPO receptors are found in cardiovascular systems including endothelial cells and cardiomyocytes (2). These findings suggest that EPO is expected to have some function in cardiovascular systems. Indeed, several investigators showed that an administration of EPO before or shortly after the onset of ischemia reduced myocardial infarct size and improved cardiac function in acute phases (3, 4). Another interesting non-erythroid function of EPO is the promotion of endothelial progenitor cell (EPC) mobilization in animals and humans, which may enhance neovascularization of ischemic areas (5, 6). Recently, Hirata et al. demonstrated that EPO increased EPC and enhances angiogenesis in ischemic myocardium after myocardial infarction (MI) and simultaneously improved cardiac function (7).

Along with these lines of evidence, Nishiya et al. importantly investigated effects of EPO on cardiac remodeling after MI in rats (8). They administered EPO in two different ways: Subcutaneous injection once a day for 4 days at 5,000 U/kg or 3 times a week for 4 weeks at 1,000 U/kg. They found that EPO improved both hemodynamic parameters and cardiac function after MI in both experimental groups. They also found that EPO prevented caspase-3 activation, up-regulation of remodeling-related genes, and the increase in interstitial fibrosis in non-infarcted myocardium. Finally, they showed enhanced angiogenesis and reduced apoptosis in the peri-infarcted myocardium. Their findings provide additional important evidence that EPO exerts cardioprotective effects after ischemia/reperfusion injury. However, if EPO is to be used in clinical applications, there are several important considerations.

Therapeutic dose and time-window

Nishiya et al. demonstrated that the administration of EPO (1,000 – 5,000 U/kg) improved cardiac function after a complete occlusion model of MI (8). The doses of EPO administered were nearly 10 times higher than those clinically used in anemic patients with chronic renal failure (1). Hirata et al. demonstrated that EPO dose-dependently (100 – 1000 IU/kg) reduced infarct size in a canine model of ischemia/reperfusion (7). Further investigation will be needed to determine the optimal dose of EPO for exerting caridoprotective effects in clinical use.

The timing for EPO administration is another important issue that must be solved to apply this agent in clinical practice. Nishiya et al. administered EPO in two different ways: Subcutaneous injection once a day for 4 days or 3 times a week for 4 weeks (8). Several investigators showed that an administration of EPO before or shortly after the onset of ischemia reduced myocardial infarct size and improved cardiac function in acute phases (3, 4). Interestingly, van der Meer et al. demonstrated that EPO started three weeks after MI increased capillary density and simultaneously improved cardiac function in rats with MI (9). Further investigations will be also needed to determine the optimal timing

*Corresponding author. kitakaze@zf6.so-net.ne.jp
Published online in J-STAGE: June 15, 2006
doi: 10.1254/jphs.LTJ06001X

and dose when EPO is applied in clinical practice.

Potential mechanisms by which EPO induces cardioprotection

Reduction of apoptotic cell death

Consistent with previous studies (3, 4), Nishiya et al. demonstrated that EPO decreased the number of TUNEL-positive cells in the peri-infarcted myocardium, suggesting that EPO prevents apoptotic cell death (8). However, since the TUNEL method also detects single strand breaks occurring in the course of necrotic cell death, it is likely that EPO attenuates apoptotic and necrotic cell death. Indeed, if EPO only inhibits the apoptotic cell death, it may be difficult to explain the marked reduction of infarct size by EPO. Recent reports suggest that EPO can inhibit the release of free radicals from neutrophils and act as a radical scavenger (1), both of which may reduce cardiac cell death after ischemia/reperfusion and attenuate cardiac remodeling.

Angiogenesis

Nishiya et al. showed enhanced angiogenesis in the peri-infarcted myocardium, which may contribute to the improvement of cardiac function after MI (8). Consistent with their report, we also found that EPO increased the number of EPC and angiogenesis in the ischemic myocardium (7). Interestingly, Nishiya et al. demonstrated that long-term administration of EPO significantly increased vessel density compared to short-term administration of EPO. Although EPO is a powerful stimulator of EPC mobilization from the bone marrow, it also has pro-angiogenetic effects (10). These different angiogenetic effects of EPO might explain the result of Nishiya's study.

Prevention of remodeling in the non-infarcted areas

Recent studies have highlighted the importance of fibrosis of non-infarcted areas remote from the site of infarction for the pathogenesis of post-infarction cardiac dysfunction (11, 12). Nishiya et al. clearly demonstrated that EPO prevented caspase-3 activation, up-regulation of remodeling-related genes, and the increase in interstitial fibrosis in non-infarcted myocardium. Prevention of cardiac remodeling in the non-infarcted myocardium will also contribute to the EPO-induced improvement of cardiac function after MI.

Clinical relevance

Recently, a higher endogenous EPO level can predict a smaller infarct size in patients with acute MI subjected to successful primary percutaneous coronary intervention (13). These findings support the idea that an administration of EPO would exert cardioprotective effects against acute ischemia reperfusion injury and cardiac remodeling. However, we must be careful of thromboembolism when we apply EPO in the clinical situation. A high dose (40,000 – 60,000 IU per week) of subcutaneously administered EPO increased the incidence of thrombotic events such a venous thrombosis or pulmonary embolisms in patients with breast cancer (14). On the other hand, in a previous clinical study, a high dose (33,000 IU once daily for the first 3 days) of intravenously administered EPO was well tolerated in patients with stroke and improved clinical outcome at 1 month (15). Careful clinical study will be warranted if EPO is to be applied for the treatment of patients with acute MI.

Although considerable future work will be required, EPO is a potentially promising candidate for an adjunctive therapy for acute MI and cardiac remodeling, and Nishiya et al. largely and importantly contributed to the paradigm of EPO in the field of cardiovascular protection.

References

1 Fisher JW. Erythropoietin: physiology and pharmacology update. Exp Biol Med (Maywood). 2003;228:1–14.

2 Wright GL, Hanlon P, Amin K, Steenbergen C, Murphy E, Arcasoy MO. Erythropoietin receptor expression in adult rat cardiomyocytes is associated with an acute cardioprotective effect for recombinant erythropoietin during ischemia-reperfusion injury. FASEB J. 2004;18:1031–1033.

3 Hirata A, Minamino T, Asanuma H, Sanada S, Fujita M, Tsukamoto O, et al. Erythropoietin just before reperfusion reduces both lethal arrhythmias and infarct size via the phosphatidylinositol-3 kinase-dependent pathway in canine hearts. Cardiovasc Drugs Ther. 2005;19:33–40.

4 Calvillo L, Latini R, Kajstura J, Leri A, Anversa P, Ghezzi P, et al. Recombinant human erythropoietin protects the myocardium from ischemia reperfusion injury and promotes beneficial remodeling. Proc Natl Acad Sci U S A. 2003;100:4802–4806.

5 Heeschen C, Aicher A, Lehmann R, Fichtlscherer S, Vasa M, Urbich C, et al. Erythropoietin is a potent physiologic stimulus for endothelial progenitor cell mobilization. Blood. 2003;102:1340–1346.

6 Bahlmann FH, DeGroot K, Duckert T, Niemczyk E, Bahlmann E, Boehm SM, et al. Endothelial progenitor cell proliferation and differentiation is regulated by erythropoietin. Kidney Int. 2003;64:1648–1652.

7 Hirata A, Minamino T, Asanuma H, Sanada S, Fujita M, Wakeno M, et al. Erythropoietin enhances neovascularization of ischemic myocardium and improves left ventricular dysfunction after myocardial infarction in dogs. Circulation. 2005;112:II–199.

8 Nishiya D, Omura T, Shimada K, Matsumoto R, Kusuyama T, Enomoto S, et al. Effects of erythropoietin on cardiac remodel-

ing after myocardial infarction. J Pharmacol Sci. 2006;101:31–39.
9 van der Meer P, Lipsic E, Henning RH, Boddeus K, van der Velden J, Voors AA, et al. Erythropoietin induces neovascularization and improves cardiac function in rats with heart failure after myocardial infarction. J Am Coll Cardiol. 2005;46:125–133.
10 Tepper OM, Capla JM, Galiano RD, Ceradini DJ, Callaghan MJ, Kleinman ME, et al. Adult vasculogenesis occurs through in situ recruitment, proliferation, and tubulization of circulating bone marrow-derived cells. Blood. 2005;105:1068–1077.
11 Jugdutt BI. Ventricular remodeling after infarction and the extracellular collagen matrix: when is enough enough? Circulation. 2003;108:1395–1403.
12 Borg TK, Ranson WF, Moslehy FA, Caulfield JB. Structural basis of ventricular stiffness. Lab Invest. 1981;44:49–54.
13 Namiuchi S, Kagaya Y, Ohta J, Shiba N, Sugi M, Oikawa M, et al. High serum erythropoietin level is associated with smaller infarct size in patients with acute myocardial infarction who undergo successful primary percutaneous coronary intervention. J Am Coll Cardiol. 2005;45:1406–1412.
14 Ehrenreich H, Hasselblatt M, Dembowski C, Cepek L, Lewczuk P, Stiefel M, et al. Erythropoietin therapy for acute stroke is both safe and beneficial. Mol Med. 2002;8:495–505.
15 Rosenzweig MQ, Bender CM, Lucke JP, Yasko JM, Brufsky AM. The decision to prematurely terminate a trial of R-HuEPO due to thrombotic events. J Pain Symptom Manage. 2004;27:185–190.

Long-Term Stimulation of Adenosine A2b Receptors Begun After Myocardial Infarction Prevents Cardiac Remodeling in Rats

Masakatsu Wakeno, MD; Tetsuo Minamino, MD, PhD; Osamu Seguchi, MD; Hidetoshi Okazaki, MD; Osamu Tsukamoto, MD, PhD; Ken-ichiro Okada, MD, PhD; Akio Hirata, MD, PhD; Masashi Fujita, MD, PhD; Hiroshi Asanuma, MD, PhD; Jiyoong Kim, MD; Kazuo Komamura, MD, PhD; Seiji Takashima, MD, PhD; Naoki Mochizuki, MD, PhD; Masafumi Kitakaze, MD, PhD

Background—Adenosine inhibits proliferation of cardiac fibroblasts and hypertrophy of cardiomyocytes, both of which may play crucial roles in cardiac remodeling. In the present study, we investigated whether chronic stimulation of adenosine receptors begun after myocardial infarction (MI) prevents cardiac remodeling.

Methods and Results—MI was produced in Wistar rats by permanent ligation of the left anterior descending coronary artery. One week after the onset of MI, animals were randomized into 8 groups: vehicle, dipyridamole (DIP; the adenosine uptake inhibitor, 50 mg/kg), 2-chroloadenosine (CADO; the stable analogue of adenosine, 2 mg/kg), and CADO in the presence of the nonselective adenosine receptor antagonist 8-sulfophenyltheophylline (8-SPT) or the selective antagonist for adenosine A1, A2a, A2b, or A3 receptor. Three weeks after treatment, hemodynamic and echocardiographic parameters in the DIP and CADO groups were significantly improved compared with the vehicle group. These hemodynamic and echocardiographic improvements were blunted by either 8-SPT or the selective adenosine A2b antagonist MRS1754 but not by the selective antagonists for other subtypes of adenosine receptors. The collagen volume fraction was smaller, and gene expression of the molecules associated with cardiac remodeling such as matrix metalloproteinase in noninfarcted areas was reduced in the DIP and CADO groups compared with the vehicle group, both of which were attenuated by either 8-SPT or MRS1754.

Conclusions—Long-term stimulation of adenosine A2b receptors begun after MI attenuates cardiac fibrosis in the noninfarcted myocardium and improves cardiac function. Drugs that stimulate adenosine A2b receptors or increase adenosine levels are new candidates for preventing cardiac remodeling after MI. (***Circulation.* 2006;114:1923-1932.**)

Key Words: adenosine ■ heart failure ■ myocardial infarction ■ remodeling

Chronic heart failure (CHF) is a major complication of myocardial infarction (MI) that substantially worsens its prognosis.[1,2] Although several major therapeutic advances have been made in the management of MI, postinfarction CHF remains a common cause of high morbidity, hospitalization, and cardiac death.[3,4] Worsening of cardiac functions after MI is followed by a complex sequence of structural changes of the left ventricle (LV), referred to as postinfarction remodeling.[3,4] These changes include progressive chamber dilatation, cardiac hypertrophy, and fibrosis.[4,5] Recent studies have highlighted the importance of fibrosis in noninfarcted areas remote from the site of infarction for the pathogenesis of postinfarction cardiac dysfunction.[3–7]

Clinical Perspective p 1932

Adenosine is a nucleoside that exerts multiple functions through specific subtypes of adenosine receptors.[8,9] Four subtypes of adenosine receptors (A1, A2a, A2b, and A3) have been cloned and pharmacologically characterized.[10,11] Adenosine triggers/mediates cardioprotection against short-term ischemia/reperfusion injury mainly through adenosine A1, A2a, and A3 receptors.[12–14] In addition, adenosine inhibits cardiac hypertrophy as a result of pressure overload through adenosine A1 receptors.[15] Adenosine also inhibits proliferation of cultured myocardial fibroblast through adenosine A2b receptors,[16] suggesting that adenosine may play an important role in cardiac remodeling. Recently, we found that plasma adenosine levels increase in patients with CHF[17] and that a further elevation of plasma adenosine levels resulting from either dipyridamole (DIP) or dilazep reduces the severity of CHF.[18] However, the long-term effects of adenosine that start after the completion of the necrotic process following MI on cardiac remodeling are unclear. Furthermore, it has

Received March 30, 2006; revision received August 22, 2006; accepted August 28, 2006.

From the Departments of Bioregulatory Medicine (M.W., O.S., H.O., N.M.) and Cardiovascular Medicine (T.M., O.T., K.-i.O., A.H., M.F., S.T.), Osaka University Graduate School of Medicine, and Divisions of Cardiovascular Medicine (M.W., O.S., H.O., H.A., K.K., J.K., M.K.) and Structural Analysis (M.W., O.S., H.O., N.M.), National Cardiovascular Center, Suita, Osaka, Japan.

Correspondence to Masafumi Kitakaze, MD, PhD, Division of Cardiovascular Medicine, National Cardiovascular Center, 5–7–1 Fujishirodai, Suita Osaka 565–8565, Japan. E-mail kitakaze@zf6.so-net.ne.jp

Circulation is available at http://www.circulationaha.org

DOI: 10.1161/CIRCULATIONAHA.106.630087

not been determined which subtypes of adenosine receptors are involved in cardiac remodeling. In the present study, we investigated whether the long-term stimulation of adenosine receptors prevents cardiac remodeling in rat MI model and, if so, which subtype of adenosine receptors are involved in this condition.

Methods

Animals

All procedures were performed in conformity with the *Guide for the Care and Use of Laboratory Animals* (NIH publication No. 85–23, 1996 revision) and were approved by the Osaka University Committee for Laboratory Animal Use.

Materials

DIP, the adenosine uptake inhibitor, was kindly provided by Boehringer-Ingelheim (Ingelheim, Germany). 2-Chroloadenosine (CADO; the stable analogue of adenosine), 8-sulfophenyltheophylline (8-SPT; the nonselective antagonist of adenosine receptors), 1,3-diethyl-8-phenylxanthine (DPCPX; the selective adenosine A1 antagonist), 5-amino-7-(phenylethyl)-2-(2-furyl)-pyrazolo[4,3-e]-1,2,4-triazolo[1,5-c] pyrimidine (SCH58261; the selective adenosine A2a antagonist), 8-[4-[((4-cyanohenyl)carbamoylmethyl)oxy]phenyl]-1, 3-di(n-propyl)xanthine (MRS1754; the selective adenosine A2b receptor antagonist), and (5-propyl-2-ethyl-4-propyl-3-(ethylsulfanylcarbonyl)-6-phenylpyridine-5-carboxylate) (MRS1523; the selective adenosine A3 receptor antagonist) were purchased from Sigma Chemical Co (St Louis, Mo). DIP, CADO, and 8-SPT were dissolved in saline. DPCPX, MRS1754, and MRS1523 were dissolved in a solution of 50% dimethyl sulfoxide in distilled water and diluted immediately before use in saline. SCH58261 was dissolved in Tween 80 aqueous suspension (5 mL/kg). Antibodies for matrix metalloproteinase (MMP)-2 and MMP-9 were purchased from Santa Cruz Biotechnology (Santa Cruz, Calif).

Experimental Protocols

Male Wistar rats (age, 8 weeks; weight, 240 to 260 g; Japan Animals, Osaka, Japan) were used in these experiments. MI was induced by permanent ligation of the left anterior descending coronary artery as previously described.[19] Briefly, the rats were anesthetized with sodium pentobarbital (30 mg/kg IP), the thorax was opened, the heart was exteriorized, and a ligature was placed around the proximal left anterior descending coronary artery. The heart was returned to its normal position, and the thorax was closed. Mortality was 47% within the first 24 hours. The same surgical procedure was performed in a sham group of rats (n=8) except that the suture around the coronary artery was not tied.

Starting on the seventh postoperative day, sham rats received 2% dimethyl sulfoxide intraperitoneally, and surviving MI rats were randomly allocated to 1 of the following 8 treatment groups: vehicle (2% dimethyl sulfoxide), DIP (50 $mg \cdot kg^{-1} \cdot d^{-1}$ PO), CADO (2 $mg \cdot kg^{-1} \cdot d^{-1}$), CADO (2 $mg \cdot kg^{-1} \cdot d^{-1}$) plus 8-SPT (10 $mg \cdot kg^{-1} \cdot d^{-1}$), CADO (2 $mg \cdot kg^{-1} \cdot d^{-1}$) plus DPCPX (0.1 $mg \cdot kg^{-1} \cdot d^{-1}$), CADO (2$mg \cdot kg^{-1} \cdot d^{-1}$) plus SCH58261 (1 $mg \cdot kg^{-1} \cdot d^{-1}$), CADO (2 $mg \cdot kg^{-1} \cdot d^{-1}$) plus MRS1754 (1 $mg \cdot kg^{-1} \cdot d^{-1}$), or CADO (2 $mg \cdot kg^{-1} \cdot d^{-1}$) plus MRS1523 (1 $mg \cdot kg^{-1} \cdot d^{-1}$); these treatments were given to MI rats (n=8, respectively) for 3 weeks. DIP was given by gastric gavage twice daily. CADO and all adenosine receptor antagonists were given intraperitoneally twice daily. The administration of CADO at the dose used in the present study (1 mg/kg IP) into sham or MI rats (n=5 for both) caused maximal decrease 5 minutes after its administration in pulse rate (24±4% and 22±6% reduction from the baseline, respectively) and systolic blood pressure (26±5% and 27±3% reduction from the baseline, respectively), both of which returned to baseline 90 minutes after the administration was discontinued. Administration of 8-SPT (5 mg/kg IP) blocked the CADO-induced hemodynamic changes. Doses of antagonists for subtypes of adenosine receptors used in the in vivo study were chosen on the basis of previous studies of their efficacy.[15,20–25]

Noninvasive Blood Pressure and Pulse Rate

Both blood pressure and pulse rate were measured before MI and 1 and 4 weeks after MI by the tail-cuff method without the use of anesthesia (MK-2000, Muromachi, Tokyo, Japan).

Echocardiographic Studies

Rats were lightly anesthetized with sodium pentobarbital anesthesia (30 mg/kg IP).[26] Echocardiography was performed using a commercially available echocardiographic system equipped with a 15-MHz phased-array transducer (SONOS 5500, Hewlett Packard, Andover, Mass). A 2-dimensional short-axis view of the LV was obtained at the level of the papillary muscles. These studies were performed at both 1 and 4 weeks after MI.

Hemodynamic Studies

LV systolic pressure (LVSP), LV end-diastolic pressure (LVEDP), maximal rate of pressure rise and decline (LV dP/dt_{max} and LV dP/dt_{min}, respectively), and heart rate were measured with a 3.5F Millar pressure catheter 4 weeks after MI under sodium pentobarbital anesthesia (30 mg/kg IP).

Histology

The right ventricle and LV were separated in ice-cold saline and weighed. The LV was cut into 3 transverse sections: apex, mid ventricle, and base. For the light microscopic study, the specimens were fixed in 10% formaldehyde, embedded in paraffin, and cut into 4-μm-thick sections, which were stained with hematoxylin and eosin and Masson's trichrome stains (n=8 for both).

Infarct size was determined as previously described.[27] Briefly, infarct size was calculated as the average of all slices stained with Masson's trichrome and expressed as a percentage of the fibrotic length to the mean LV circumference. Rats with an infarct size <30% were excluded from analysis because they did not show typical LV remodeling.

The cross-sectional area of cardiomyocytes was measured as previously described.[26] One hundred cardiomyocytes per heart stained with hematoxylin and eosin were counted, and the average area was determined.

The collagen volume fraction was measured while omitting fibrosis of the perivascular, epicardial, and endocardial areas.[26] The collagen volume fraction was expressed as the average of connective tissue to the total tissue area of all slices stained with Masson's trichrome.

Quantitative Real-Time Reverse-Transcriptase Polymer Chain Reaction

Quantitative real-time reverse-transcriptase polymer chain reaction was performed as described previously.[28] Total RNA from the noninfarcted and infracted LV was extracted with RNA-Bee-RNA Isolation Reagent (Tel-Test, Friendswood, Tex). Then, 200 ng total RNA was reverse transcribed and amplified with an Omniscript RT Kit (Qiagen, Hilden, Germany) according to the manufacturer's protocol. Oligonucleotide primers and TaqMan probes for rat collagen type I, rat collagen type III, rat transforming growth factor-β1 (TGF-β1), rat MMP-2, rat MMP-9, rat tissue inhibitor of metalloproteinase (TIMP)-1, TIMP-2, rat atrial natriuretic factor (ANF), rat brain natriuretic peptide (BNP), and rodent glyceraldehyde phosphate dehydrogenase were purchased from Applied Biosystems (Forster City, Calif).

Immunoblotting

Immunoblotting was performed as described previously.[28] Immunoreactive bands were quantified by densitometry (Molecular Dynamics).

Collagen Synthesis in Cultured Cardiac Fibroblasts

Adult cardiac fibroblasts were prepared as described previously.[16] The effects of either DIP or CADO on collagen synthesis in cardiac fibroblasts were evaluated on confluent cultures by incorporating [^{3}H]proline into cells as previously described.[29] Then, either DIP or CADO with or without antagonists for subtypes of adenosine A1, A2a, A2b, or A3 receptors was added; [^{3}H]proline (0.5 μCi/mL) also was added. After the cells were incubated for 24 hours, the radioactivity of aliquots of the trichloroacetic acid–insoluble material was determined with a liquid scintillation counter. Cardiac fibroblasts in the first or second passage were used for all experiments. Doses of antagonist for subtypes of adenosine receptors used in the in vitro study were chosen on the basis of previous studies of their efficacy.[11,16]

Statistical Analysis

All data are expressed as mean±SEM. Comparisons of the time course changes between groups were performed by use of 2-way repeated-measures ANOVA. Comparisons of other data between groups were performed through the use of 1-way fractional ANOVA. The Bonferroni-Holm procedure was used to correct multiple comparisons. A value of $P<0.05$ was considered statistically significant.

The authors had full access to the data and take full responsibility for their integrity. All authors have read and agree to the manuscript as written.

Results

Effects of Adenosine and Antagonists for Subtypes of Adenosine Receptors on Infarct Size and Hemodynamic Parameters

Both blood pressure (110±8 mm Hg) and pulse rate (405±11 bpm) under baseline conditions in the sham group did not change throughout the protocol and were not different at any time points compared with the MI groups. In addition, body weight at baseline (250±5 g) and at the end of the protocol (424±3 g) did not differ from other groups. No difference in infarct size among groups tested was found (Figure 1).

Four weeks after the onset of MI, LVEDP in all MI groups was higher than in the sham group (Figure 2A). Both LV dP/dt_{max} and LV dP/dt_{min} in all MI groups were smaller than in the sham group (Figure 2B and 2C). Long-term adenosine receptor stimulation by either DIP or CADO decreased LVEDP and increased both LV dP/dt_{max} and LV dP/dt_{min}. The improvement in hemodynamic parameters as a result of CADO treatment was blunted by 8-SPT or MRS1754 but not by other antagonists for subtypes of adenosine receptors (Figure 2A through 2C). No statistical difference existed in LVSP (Figure 2D) or heart rate (sham, 372±8 bpm) among all groups when hemodynamic parameters such as LVEDP, LV dP/dt_{max}, and LV dP/dt_{min} were measured. The ratios of heart weight to body weight, ventricular weight to body weight, and lung weight to body weight increased in all MI groups compared with the sham group. Long-term stimulation of adenosine receptors by CADO decreased all 3 ratios compared with other MI groups (the Table). Either 8-SPT or MRS1754, but not the antagonist for other subtypes of adenosine receptors, blunted the decrease in all 3 ratios by CADO.

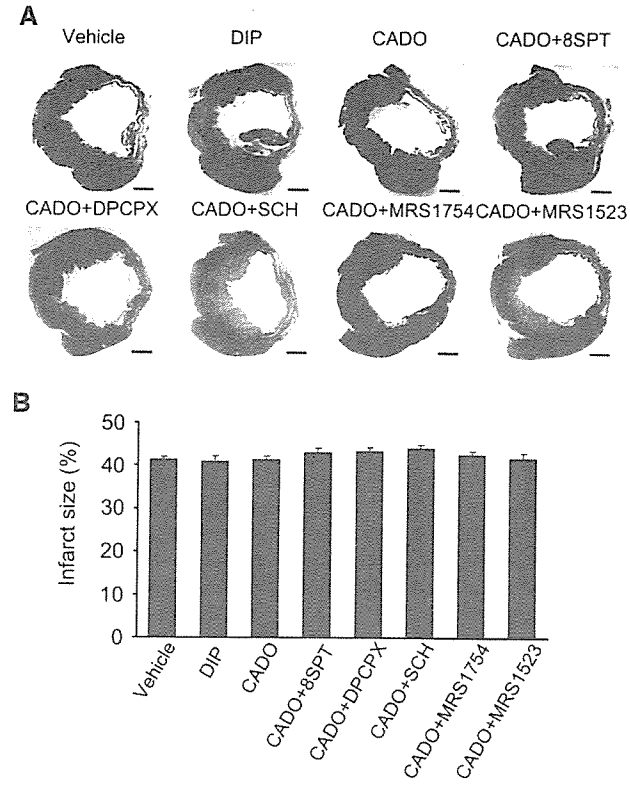

Figure 1. Effects of adenosine and antagonists for subtypes of adenosine receptors on infarct size. A, Representative LV cross sections. Scale bar=1 mm. B, Quantitative analysis of myocardial infarct size. Values are mean±SEM. No statistical difference was found among all groups (n=8).

Effects of Adenosine and the Antagonists for Subtypes of Adenosine Receptors on Echocardiographic Parameters

Figure 3A shows the M-mode view of all groups. Four weeks after the onset of MI, both LV end-diastolic dimension and LV end-systolic dimension in all MI groups were larger than in the sham group. Although no statistical difference existed in LV end-diastolic dimension among MI groups, both DIP and CADO reduced LV end-systolic dimension and increased fractional shortening. The improvement in echocardiographic parameters by CADO was blunted by either 8-SPT or MRS1754 but not by the antagonist for other subtypes of adenosine receptors (Figure 3B).

Effects of Adenosine and Antagonists for Subtypes of Adenosine Receptors on Cardiac Collagen Volume in Noninfarcted Areas

To clarify the pathophysiological mechanism of the improved cardiac performance caused by the long-term stimulation of adenosine receptors by either DIP or CADO, we examined the collagen volume fraction in noninfarcted areas that may affect cardiac remodeling. The collagen volume fraction in all MI groups increased more than in the sham group, and administration of either DIP or CADO attenuated an increase in morphometric collagen volume fraction in noninfarcted areas (Figure 4). Either 8-SPT or

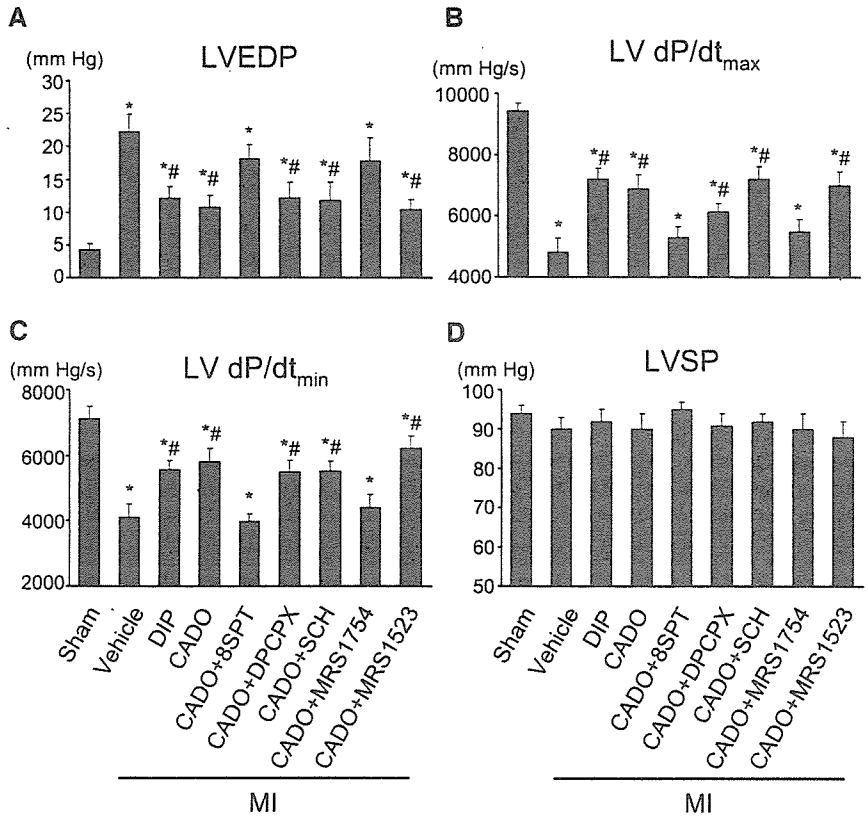

Figure 2. Effects of adenosine and antagonists for subtypes of adenosine receptors on hemodynamic parameters. A, LVEDP; B, LV dP/dt_{max}; C, LV dP/dt_{min}; D, LVSP. Values are mean±SEM. *$P<0.05$ vs sham; #$P<0.05$ vs vehicle (n=8).

MRS1754, but not antagonists for other subtypes of adenosine receptors, abolished the effects of CADO on the collagen volume fraction in the noninfarcted areas. CADO (93±4%) or DIP (90±5%) did not change the collagen volume fraction in infracted areas compared with vehicle (88±4%).

Effects of Adenosine and Antagonists for Subtypes of Adenosine Receptors on Cardiac Hypertrophy in Noninfarcted Areas

The cross-sectional area of cardiomyocytes in all MI groups increased more than in the sham group, and either DIP or CADO inhibited hypertrophy of cardiomyocytes in noninfarcted areas (Figure 5). Either 8-SPT or DPCPX, but not other adenosine receptor antagonists, abolished the effects of CADO on hypertrophy of cardiomyocytes.

Effects of Antagonists for Subtypes of Adenosine Receptors on Molecules Associated With Cardiac Remodeling in Noninfarcted Areas

To examine the molecular mechanisms by which adenosine attenuates cardiac fibrosis in the noninfarcted myocardium, we examined the mRNA levels of molecules associated with fibrosis and hypertrophy in noninfarcted areas after MI (Figure 6). The increased mRNA expressions of collagen type I, TGF-β1, MMP-2, and TIMP-1 after MI were suppressed by treatment with either DIP or CADO. Interestingly, either 8-SPT or MRS1754, but not the antagonist for other subtypes

Heart Weight and Lung Weight 4 Weeks After MI

		MI							
	Sham	Vehicle	DIP	CADO	CADO+8SPT	CADO+DPCPX	CADO+SCH58261	CADO+MRS1754	CADO+MRS1523
HW/BW, mg/g	2.93±0.06	4.05±0.11*	3.52±0.15*†	3.60±0.11*†	3.95±0.12*	3.58±0.09*†	3.51±0.12*†	3.89±0.06*	3.45±0.19*†
VW/BW, mg/g	2.54±0.06	3.65±0.11*	3.25±0.09*†	3.21±0.10*†	3.54±0.11*	3.17±0.08*†	3.11±0.12*†	3.48±0.07*	3.05±0.19*†
LVW/BW, mg/g	1.93±0.07	2.57±0.07*	2.62±0.12*	2.60±0.10*	2.60±0.17*	2.56±0.10*	2.50±0.11*	2.48±0.09*	2.47±0.19*
LW/BW, mg/g	3.3±0.10	8.2±1.0*	4.8±0.4*†	4.4±0.2*†	8.8±0.7*	5.1±0.4*†	4.4±0.6*†	7.7±0.7*	4.2±0.3*†

HW indicates heart weight; BW, body weight; VW, ventricular weight; LVW, LV weight; and LW, lung weight. Values are mean±SEM (n=8).
*$P<0.05$ vs sham.
†$P<0.05$ vs vehicle.

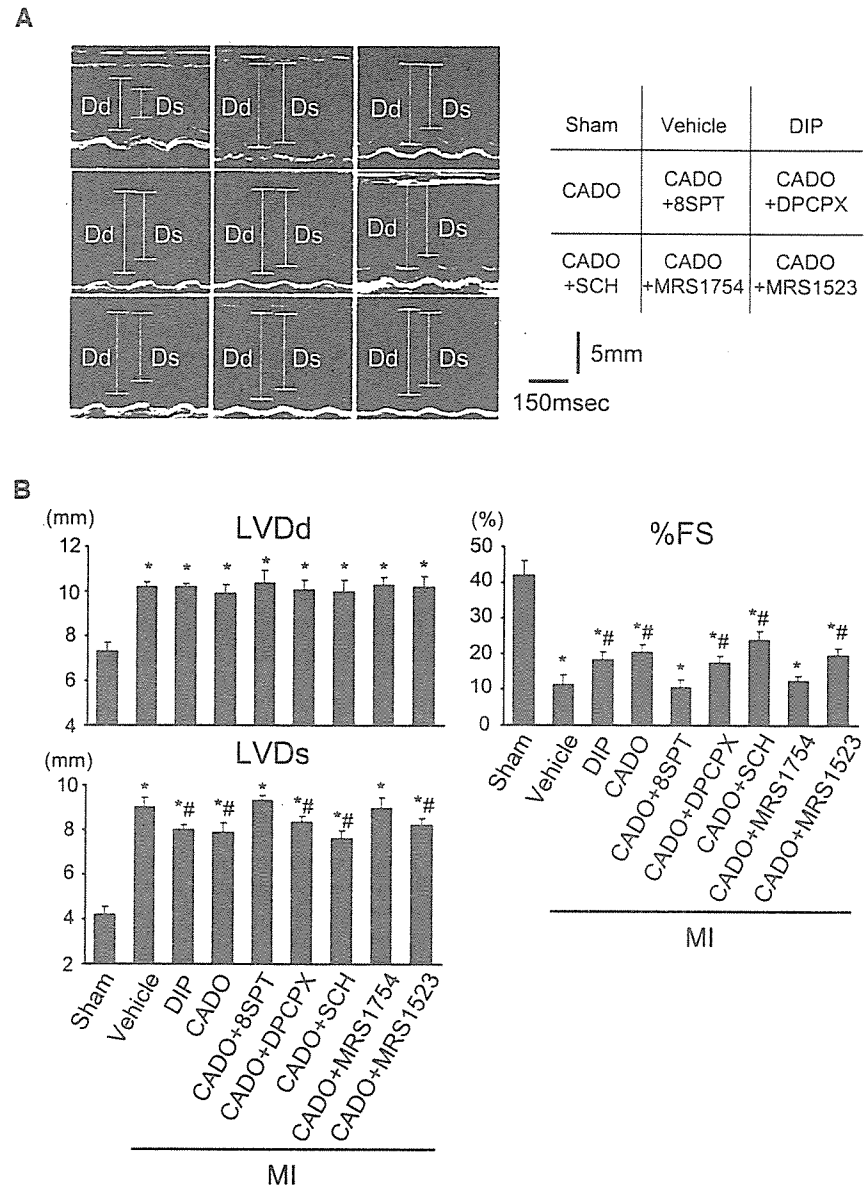

Figure 3. Effects of adenosine and antagonists for subtypes of adenosine receptors on echocardiographic parameters. A, Representative 2D echocardiograms. B, Quantitative analysis of echocardiographic parameters. Values are mean±SEM. LVDd indicates LV end-diastolic dimension; LVDs, LV end-systolic dimension; and %FS, fractional shortening. *$P<0.05$ vs sham; #$P<0.05$ vs vehicle (n=8).

of adenosine receptors, blunted the suppression of mRNA levels of collagen type I, TGF-β1, MMP-2, or TIMP-1 by CADO. However, neither DIP nor CADO changed the mRNA levels of MMP-9 or TIMP-2, each of which may also link with cardiac remodeling after MI.[30] Consistent with the mRNA levels of MMP-2 and MMP-9, CADO decreased MMP-2, but not MMP-9, protein levels in noninfarcted areas (Figure 7). Either DIP or CADO treatment resulted in suppression of the ANF and BNP mRNA levels, both of which are useful markers of cardiac hypertrophy, in noninfarcted areas (Figure 6G and 6H). 8-SPT or DPCPX, but not the antagonist for other subtypes of adenosine receptors, blunted the suppression of mRNA levels of ANF by CADO. 8-SPT, DPCPX, or MRS1754, but not the antagonist for other subtype of adenosine receptors, blunted the suppression of mRNA levels of BNP by CADO. In infarcted areas, all of the evaluated molecules increased in all MI groups compared with the sham group, but no difference existed in expression levels among MI groups (data not shown).

Cellular Mechanisms of the Antifibrosis Action of Adenosine

Both DIP and CADO decreased the incorporation of [^{3}H]proline into cardiac fibroblasts from rat adult rats in a dose-dependent manner, either of which was blocked by 8-SPT (Figure 8A). The decrease in [^{3}H]proline incorporation by CADO was completely blocked by MRS1754, a selective adenosine A2b receptor antagonist, at a concentration of 10^{-7} mol/L (Figure 8B). DPCPX, SCH58261, or MRS1523 at a dose from 10^{-8} to 10^{-6} mol/L did not affect the reduction in [^{3}H]proline incorporation by CADO (10^{-6} mol/L) (data not shown).

Discussion

Adenosine or adenosine receptor agonist administration before the onset of ischemia or during early reperfusion has been documented by several investigators not only to reduce infarct size but also to improve functional recovery after MI.[31–33] In the present study, we demonstrated that

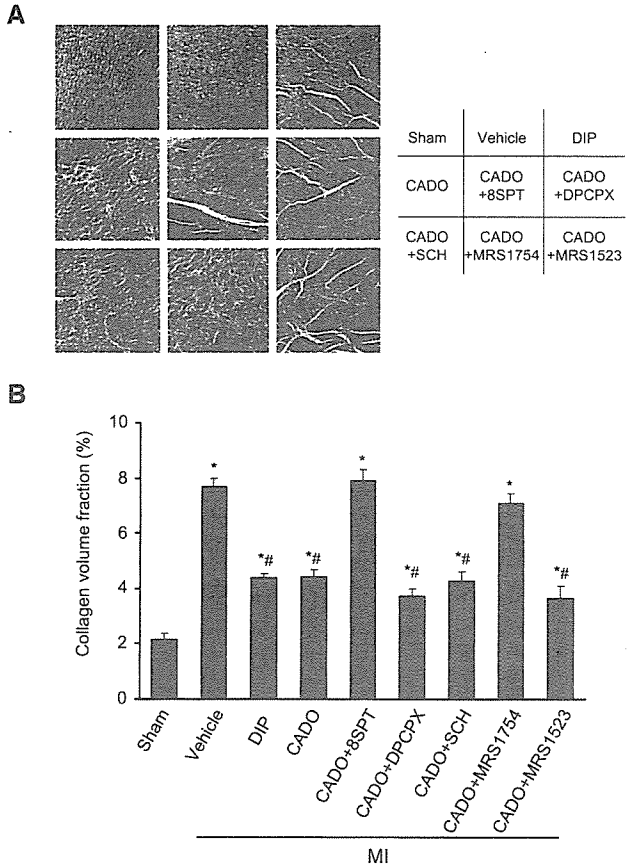

Figure 4. Effects of adenosine and antagonists for subtypes of adenosine receptors on cardiac collagen volume fraction in noninfarcted areas. A, Representative histological findings stained with Masson's trichrome in noninfarcted areas. Scale bar=200 μm. B, Quantitative analysis of collagen volume fraction in noninfarcted areas. Values are mean±SEM. *$P<0.05$ vs sham; #$P<0.05$ vs vehicle (n=8).

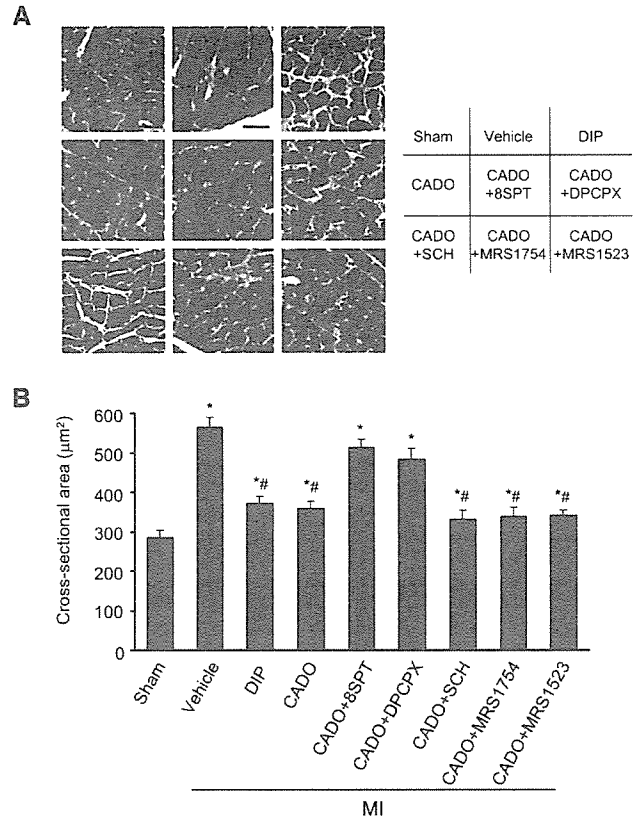

Figure 5. Effects of adenosine and antagonists for subtypes of adenosine receptors on cardiac hypertrophy in noninfarcted areas. A, Representative histological findings of cardiomyocytes stained with hematoxylin and eosin in noninfarcted areas. Scale bar=20 μm. B, Quantitative analysis of cross-sectional areas of cardiomyocyte. Values are mean±SEM. *$P<0.05$ vs sham; #$P<0.05$ vs vehicle (n=8).

the long-term administration of either DIP or CADO that starts 1 week after the onset of MI, during which time the necrotic process may be completed,[34] improves cardiac performance in MI rats, as indicated by hemodynamic and echocardiographic parameters. To the best of our knowledge, this study is the first to document that adenosine administered after the completion of the necrotic process exerts cardioprotective effects.

We also demonstrated that the attenuation of cardiac remodeling by adenosine was blunted by 8-SPT, indicating that the activation of adenosine receptors is responsible for the attenuation of cardiac remodeling after MI. Importantly, we further examined which subtype of adenosine receptor was involved in cardiac remodeling after MI. Because 4 subtypes of adenosine receptors have been cloned in the rat,[9,10] we used specific antagonists for subtypes of adenosine receptors: DPCPX for A1 adenosine receptors, A2a for SCH58161, A2b for MRS1754, and A3 for MRS1523.[20,22–25,35]

We found that the improvement in cardiac performance by long-term stimulation by CADO was blunted by MRS1754 but not by the antagonist of other subtypes of adenosine receptors. To the best of our knowledge, this study was the first to demonstrate the involvement of adenosine A2b receptor in cardiac remodeling.

Because the excess deposition of extracellular matrix proteins in noninfarcted areas has gained recognition as an important contributor to adverse remodeling and ventricular dysfunction after MI,[36,37] we have examined the in vivo effects of either DIP or CADO on the extent of fibrosis in noninfarcted areas. We found that either DIP or CADO significantly attenuates an increase in morphometric collagen volume fraction in noninfarcted areas. The attenuation in collagen volume fraction in noninfarcted areas by either DIP or CADO was blunted by 8-SPT or MRS1754 but not by the antagonist of other subtypes of adenosine receptors. The amount of myocardial collagen deposition after MI in infarcted and noninfarcted areas during the healing process was reported to influence and to be integral to the process of ventricular remodeling.[38] In addition, it has been shown that excessive accumulation of myocardial collagen may result in rigidity of the myocardium and severely impaired relaxation.[39] Our data strongly suggest that the reduction in collagen volume in noninfarcted areas through adenosine A2b receptors may contribute to the improvement in cardiac function after MI.

Multiple subtypes of adenosine receptors have been reported to contribute to the antihypertrophic effects of

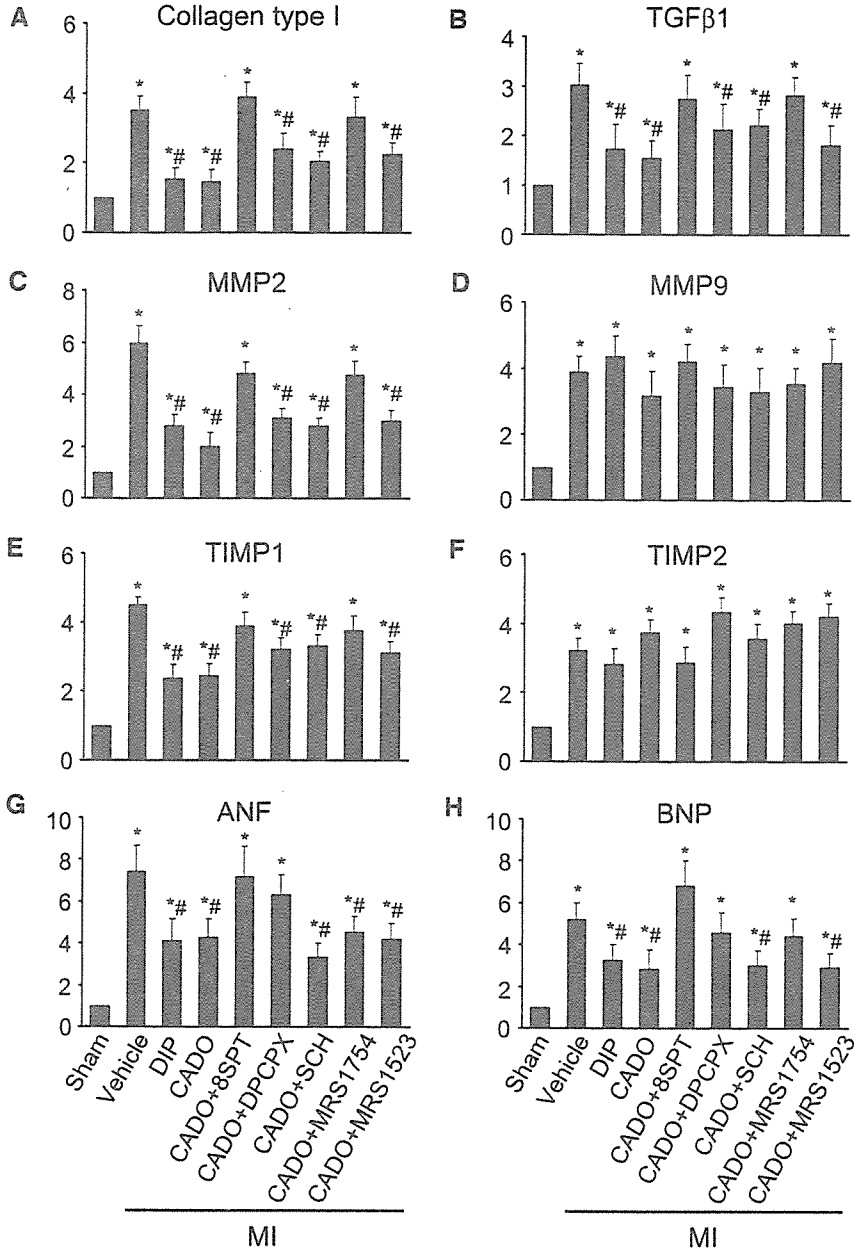

Figure 6. Effects of adenosine and antagonists for subtypes of adenosine receptors on molecules associated with cardiac remodeling in noninfarcted areas. Quantitative real-time reverse-transcriptase polymerase chain reaction analysis of collagen type I (A), TGF-β1 (B), MMP-2 (C), MMP-9 (D), TIMP-1 (E), TIMP-2 (F), ANF (G), and BNP (H). Each mRNA value was corrected for glyceraldehyde phosphate dehydrogenase mRNA value. Levels in sham group were arbitrarily assigned a value of 1.0. Values are mean±SEM. *$P<0.05$ vs sham; #$P<0.05$ vs vehicle. Results represent analysis of 3 independent experiments.

adenosine in cardiomyocytes.[40] We have recently demonstrated that adenosine inhibits cardiac hypertrophy through adenosine A1 receptor in pressure-overloaded hearts.[15] Interestingly, we found that either DIP or CADO attenuated hypertrophic changes in cardiomyocytes and mRNA levels of ANF and BNP in the noninfarcted LV, both of which were blunted by DPCPX, the antagonist of adenosine A1 receptors. However, DPCPX did not blunt the improvement in cardiac performance after MI by long-term stimulation of adenosine receptors during the experimental period, suggesting that long-term stimulation of the adenosine A1 receptor may not play an important role in cardiac remodeling after MI. One potential explanation for the discrepancy in the effects of adenosine A1 and A2 receptors on cardiac function is the difference in the pathophysiology in hearts, ie, hypertrophy versus MI. We need to consider the possibility that the long-term stimulation of adenosine A1 receptor may attenuate cardiac remodeling through its effects on cardiomyocytes.

To examine the molecular mechanism by which adenosine attenuates cardiac fibrosis in noninfarcted areas, we examined the gene expression of molecules associated with cardiac remodeling such as TGF-β1, collagen, MMPs, and TIMPs. CADO attenuated the expression of collagen type I, TGF-β1, MMP-2, and TIMP-1 in noninfarcted areas at 4 weeks after MI. In addition, the effect of CADO was blunted by either 8-SPT or MRS1754 but not by the antagonist of other subtypes of adenosine receptors. These results provide in vivo evidence that adenosine is a potent "fibrosis-inhibitory agent" after MI. Interestingly, either DIP or CADO failed to attenuate the mRNA levels of MMP-9 or TIMP-2. However, because the extracellular

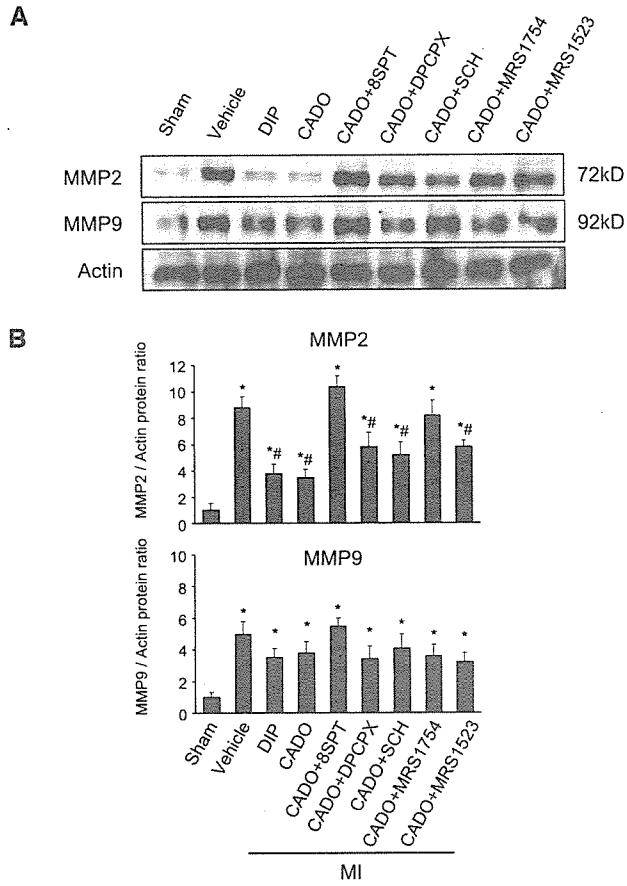

Figure 7. Effects of adenosine and antagonists for subtypes of adenosine receptors on MMP protein levels in noninfarcted areas. A, Representative immunoblot analysis of MMP-2 and MMP-9 proteins. B, Quantitative analysis of MMP-2 and MMP-9 proteins by densitometry. Each protein value was corrected for actin protein value. Levels in sham group were arbitrarily assigned a value of 1.0. Values are mean±SEM. *$P<0.05$ vs sham; #$P<0.05$ vs vehicle. Results represent analysis of 3 independent experiments.

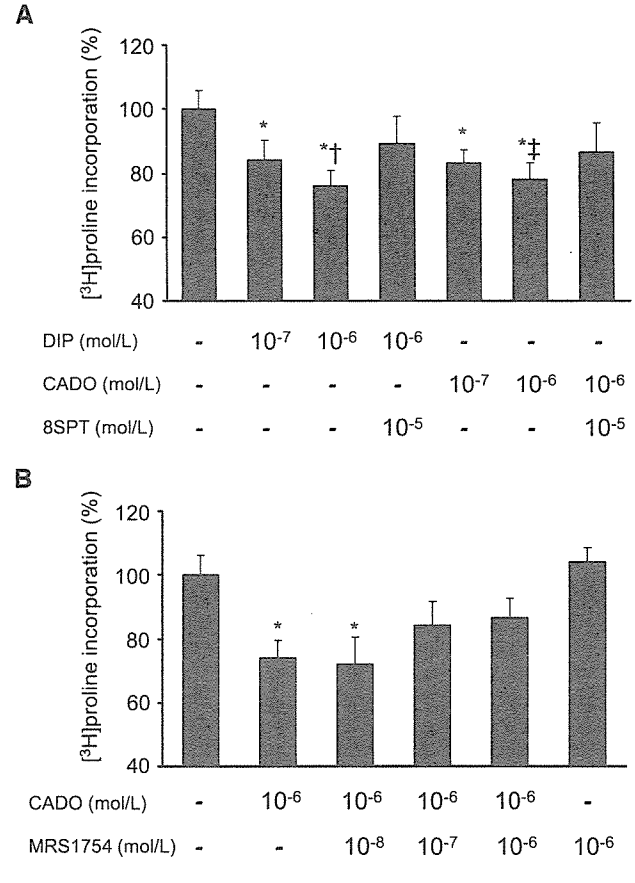

Figure 8. Cellular mechanism of the antifibrosis action of adenosine. A, The effect of DIP or CADO on [^{3}H]proline incorporation in adult cardiac fibroblasts with or without 8-SPT (10^{-5} mol/L). Results represent analysis of 3 independent experiments. B, [^{3}H]proline incorporation into adult cardiac fibroblasts with or without MSR1754, the selective A2b receptor antagonist, in the presence of CADO (10^{-6} mol/L). Values are mean±SEM. *$P<0.05$ vs no treatment; †$P<0.05$ vs DIP (10^{-7} mol/L); ‡$P<0.05$ vs CADO (10^{-7} mol/L).

matrix dramatically changes during the time course after MI,[41] we need to carefully consider the effects of adenosine on the molecules associated with cardiac remodeling. Further investigation is needed to clarify the effect of adenosine on the regulation of extracellular matrix after MI.

The activation of adenosine A2b receptors directly inhibits collagen production[42] and mitogenesis in cardiac fibroblasts from adult rats.[43,44] Consistent with the previous study,[42] our in vitro study using rat adult cardiac fibrosis showed that the decrease in [^{3}H]proline incorporation by either DIP or CADO was completely blocked by MRS1754, the selective A2b receptor antagonist, but not the antagonist of other subtypes of adenosine receptors. These findings support the idea that the activation of adenosine A2b receptors decreases the severity of myocardial fibrosis in the noninfarcted LV. Although we chose the specific antagonist for the each subtype of adenosine receptors, we must notice that these antagonists still have capacity to antagonize other subtype of adenosine receptors.[22,45] Future studies using genetically engineered animals are needed to clarify the exact role of each subtype of adenosine receptors.

The cause of CHF may not be unique, and several neurohumoral factors contribute largely to the pathophysiology of CHF.[3,4] Therefore, it is important in the treatment of CHF to attenuate these neurohumoral factors. Because adenosine is reported to attenuate the sympathetic nervous system, renin-angiotensin system, and cytokine system,[46–49] elevation of adenosine levels may contribute largely to the beneficial treatment of CHF by modulating neurohumoral factors. Recently, Yang et al[50] demonstrated the augmentation of proinflammatory cytokines such as TNFα in adenosine A2b receptor knockout mice. Further studies are needed to determine the contribution ratio of direct and indirect effects of adenosine A2b receptor on cardiac remodeling.

A number of therapeutic approaches to limiting ventricular remodeling in MI have been reported.[3,4] These agents include angiotensin-converting enzyme inhibitors, angiotensin II type 1 receptor blockers, β-adrenergic blockers, aldosterone antagonists, and MMP inhibitors.[3–5] Our findings suggest that the increased adenosine levels in CHF

may be compensatory against CHF, leading to the idea that further elevation of adenosine levels or long-term stimulation of adenosine A2b receptors may be a new strategy for treating CHF.

Acknowledgments

The authors thank Akiko Ogai and Tomoko Morita for their excellent technical assistance.

Sources of Funding

This study was supported by Grants on Scientific Research from the Japanese Ministry of Education, Culture, Sports, Science and Technology (No. 12470153 and 12877107); grants from Human Genome Tissue Engineering and Food Biotechnology (H13-genome-11); and Grants on Comprehensive Research on Aging and Health [H13–21seiki(seikatsu)-23] in Health and Labor Science Research from the Ministry of Health, Labor, and Welfare, Japan.

Disclosures

None.

References

1. Wolk MJ, Scheidt S, Killip T. Heart failure complicating acute myocardial infarction. *Circulation.* 1972;45:1125–1138.
2. Hammermeister KE, DeRouen TA, Dodge HT. Variables predictive of survival in patients with coronary disease: selection by univariate and multivariate analyses from the clinical, electrocardiographic, exercise, arteriographic, and quantitative angiographic evaluations. *Circulation.* 1979;59:421–430.
3. Jessup M, Brozena S. Heart failure. *N Engl J Med.* 2003;348: 2007–2018.
4. McMurray JJ, Pfeffer MA. Heart failure. *Lancet.* 2005;365: 1877–1889.
5. Opie LH, Commerford PJ, Gersh BJ, Pfeffer MA. Controversies in ventricular remodelling. *Lancet.* 2006;367:356–367.
6. Jugdutt BI. Ventricular remodeling after infarction and the extracellular collagen matrix: when is enough enough? *Circulation.* 2003; 108:1395–1403.
7. Cleutjens JP, Verluyten MJ, Smiths JF, Daemen MJ. Collagen remodeling after myocardial infarction in the rat heart. *Am J Pathol.* 1995;147:325–338.
8. Donato M, Gelpi RJ. Adenosine and cardioprotection during reperfusion: an overview. *Mol Cell Biochem.* 2003;251:153–159.
9. Minamino T, Kitakaze M. Cellular mechanisms for the treatment of chronic heart failure: the nitric oxide- and adenosine-dependent pathways. *Expert Opin Emerg Drugs.* 2002;7:99–110.
10. Yaar R, Jones MR, Chen JF, Ravid K. Animal models for the study of adenosine receptor function. *J Cell Physiol.* 2005;202:9–20.
11. Moro S, Gao ZG, Jacobson KA, Spalluto G. Progress in the pursuit of therapeutic adenosine receptor antagonists. *Med Res Rev.* 2006;26: 131–159.
12. Reichelt ME, Willems L, Molina JG, Sun CX, Noble JC, Ashton KJ, Schnermann J, Blackburn MR, Headrick JP. Genetic deletion of the A1 adenosine receptor limits myocardial ischemic tolerance. *Circ Res.* 2005;96:363–367.
13. Toufektsian MC, Yang Z, Prasad KM, Overbergh L, Ramos SI, Mathieu C, Linden J, French BA. Stimulation of A2A-adenosine receptors after myocardial infarction suppresses inflammatory activation and attenuates contractile dysfunction in the remote left ventricle. *Am J Physiol Heart Circ Physiol.* 2006;290:H1410–H1418.
14. Tracey WR, Magee WP, Oleynek JJ, Hill RJ, Smith AH, Flynn DM, Knight DR. Novel N6-substituted adenosine 5′-*N*-methyluronamides with high selectivity for human adenosine A3 receptors reduce ischemic myocardial injury. *Am J Physiol Heart Circ Physiol.* 2003;285: H2780–H2787.
15. Liao Y, Takashima S, Asano Y, Asakura M, Ogai A, Shintani Y, Minamino T, Asanuma H, Sanada S, Kim J, Ogita H, Tomoike H, Hori M, Kitakaze M. Activation of adenosine A1 receptor attenuates cardiac hypertrophy and prevents heart failure in murine left ventricular pressure-overload model. *Circ Res.* 2003;93:759–766.
16. Dubey RK, Gillespie DG, Jackson EK. Adenosine inhibits collagen and protein synthesis in cardiac fibroblasts: role of A2B receptors. *Hypertension.* 1998;31:943–948.
17. Funaya H, Kitakaze M, Node K, Minamino T, Komamura K, Hori M. Plasma adenosine levels increase in patients with chronic heart failure. *Circulation.* 1997;95:1363–1365.
18. Kitakaze M, Minamino T, Node K, Koretsune Y, Komamura K, Funaya H, Kuzuya T, Hori M. Elevation of plasma adenosine levels may attenuate the severity of chronic heart failure. *Cardiovasc Drugs Ther.* 1998;12:307–309.
19. Matsumoto R, Yoshiyama M, Omura T, Kim S, Nakamura Y, Izumi Y, Akioka K, Iwao H, Takeuchi K, Yoshikawa J. Effects of aldosterone receptor antagonist and angiotensin II type I receptor blocker on cardiac transcriptional factors and mRNA expression in rats with myocardial infarction. *Circ J.* 2004;68:376–382.
20. Bryan PT, Marshall JM. Adenosine receptor subtypes and vasodilatation in rat skeletal muscle during systemic hypoxia: a role for A1 receptors. *J Physiol.* 1999;514(pt 1):151–162.
21. Picano E, Michelassi C. Chronic oral dipyridamole as a "novel" antianginal drug: the collateral hypothesis. *Cardiovasc Res.* 1997;33: 666–670.
22. Hannon JP, Tigani B, Wolber C, Williams I, Mazzoni L, Howes C, Fozard JR. Evidence for an atypical receptor mediating the augmented bronchoconstrictor response to adenosine induced by allergen challenge in actively sensitized Brown Norway rats. *Br J Pharmacol.* 2002;135:685–696.
23. Monopoli A, Casati C, Lozza G, Forlani A, Ongini E. Cardiovascular pharmacology of the A2A adenosine receptor antagonist, SCH 58261, in the rat. *J Pharmacol Exp Ther.* 1998;285:9–15.
24. Kim YC, Ji X, Melman N, Linden J, Jacobson KA. Anilide derivatives of an 8-phenylxanthine carboxylic congener are highly potent and selective antagonists at human A(2B) adenosine receptors. *J Med Chem.* 2000;43:1165–1172.
25. Kin H, Zatta AJ, Lofye MT, Amerson BS, Halkos ME, Kerendi F, Zhao ZQ, Guyton RA, Headrick JP, Vinten-Johansen J. Postconditioning reduces infarct size via adenosine receptor activation by endogenous adenosine. *Cardiovasc Res.* 2005;67:124–133.
26. Soeki T, Kishimoto I, Okumura H, Tokudome T, Horio T, Mori K, Kangawa K. C-type natriuretic peptide, a novel antifibrotic and antihypertrophic agent, prevents cardiac remodeling after myocardial infarction. *J Am Coll Cardiol.* 2005;45:608–616.
27. Spitznagel H, Chung O, Xia Q, Rossius B, Illner S, Jahnichen G, Sandmann S, Reinecke A, Daemen MJ, Unger T. Cardioprotective effects of the Na(+)/H(+)-exchange inhibitor cariporide in infarct-induced heart failure. *Cardiovasc Res.* 2000;46:102–110.
28. Tsukamoto O, Minamino T, Okada K, Shintani Y, Takashima S, Kato H, Liao Y, Okazaki H, Asai M, Hirata A, Fujita M, Asano Y, Yamazaki S, Asanuma H, Hori M, Kitakaze M. Depression of proteasome activities during the progression of cardiac dysfunction in pressure-overloaded heart of mice. *Biochem Biophys Res Commun.* 2006;340:1125–1133.
29. Horio T, Tokudome T, Maki T, Yoshihara F, Suga S, Nishikimi T, Kojima M, Kawano Y, Kangawa K. Gene expression, secretion, and autocrine action of C-type natriuretic peptide in cultured adult rat cardiac fibroblasts. *Endocrinology.* 2003;144:2279–2284.
30. Sun Y, Zhang JQ, Zhang J, Lamparter S. Cardiac remodeling by fibrous tissue after infarction in rats. *J Lab Clin Med.* 2000;135: 316–323.
31. Villarreal F, Zimmermann S, Makhsudova L, Montag AC, Erion MD, Bullough DA, Ito BR. Modulation of cardiac remodeling by adenosine: in vitro and in vivo effects. *Mol Cell Biochem.* 2003;251:17–26.
32. Tsuchida A, Liu GS, Wilborn WH, Downey JM. Pretreatment with the adenosine A1 selective agonist, 2-chloro-N6-cyclopentyladenosine (CCPA), causes a sustained limitation of infarct size in rabbits. *Cardiovasc Res.* 1993;27:652–656.
33. Baxter GF, Marber MS, Patel VC, Yellon DM. Adenosine receptor involvement in a delayed phase of myocardial protection 24 hours after ischemic preconditioning. *Circulation.* 1994;90:2993–3000.
34. Reimer KA, Lowe JE, Rasmussen MM, Jennings RB. The wavefront phenomenon of ischemic cell death, 1: myocardial infarct size vs duration of coronary occlusion in dogs. *Circulation.* 1977;56: 786–794.

35. Zatta AJ, Matherne GP, Headrick JP. Adenosine receptor-mediated coronary vascular protection in post-ischemic mouse heart. *Life Sci.* 2006;78:2426–2437.
36. Weber KT. Extracellular matrix remodeling in heart failure: a role for de novo angiotensin II generation. *Circulation.* 1997;96:4065–4082.
37. Hirayama A, Kusuoka H, Yamamoto H, Sakata Y, Asakura M, Higuchi Y, Mizuno H, Kashiwase K, Ueda Y, Okuyama Y, Hori M, Kodama K. Serial changes in plasma brain natriuretic peptide concentration at the infarct and non-infarct sites in patients with left ventricular remodelling after myocardial infarction. *Heart.* 2005;91: 1573–1577.
38. Jugdutt BI, Joljart MJ, Khan MI. Rate of collagen deposition during healing and ventricular remodeling after myocardial infarction in rat and dog models. *Circulation.* 1996;94:94–101.
39. Doering CW, Jalil JE, Janicki JS, Pick R, Aghili S, Abrahams C, Weber KT. Collagen network remodelling and diastolic stiffness of the rat left ventricle with pressure overload hypertrophy. *Cardiovasc Res.* 1988;22:686–695.
40. Gan XT, Rajapurohitam V, Haist JV, Chidiac P, Cook MA, Karmazyn M. Inhibition of phenylephrine-induced cardiomyocyte hypertrophy by activation of multiple adenosine receptor subtypes. *J Pharmacol Exp Ther.* 2005;312:27–34.
41. Lindsey ML. MMP induction and inhibition in myocardial infarction. *Heart Fail Rev.* 2004;9:7–19.
42. Chen Y, Epperson S, Makhsudova L, Ito B, Suarez J, Dillmann W, Villarreal F. Functional effects of enhancing or silencing adenosine A2b receptors in cardiac fibroblasts. *Am J Physiol Heart Circ Physiol.* 2004;287:H2478–H2486.
43. Dubey RK, Gillespie DG, Zacharia LC, Mi Z, Jackson EK. A(2b) receptors mediate the antimitogenic effects of adenosine in cardiac fibroblasts. *Hypertension.* 2001;37:716–721.
44. Dubey RK, Gillespie DG, Mi Z, Jackson EK. Adenosine inhibits PDGF-induced growth of human glomerular mesangial cells via A(2B) receptors. *Hypertension.* 2005;46:628–634.
45. Kim SA, Marshall MA, Melman N, Kim HS, Muller CE, Linden J, Jacobson KA. Structure-activity relationships at human and rat A2B adenosine receptors of xanthine derivatives substituted at the 1-, 3-, 7-, and 8-positions. *J Med Chem.* 2002;45:2131–2138.
46. Hori M, Kitakaze M. Adenosine, the heart, and coronary circulation. *Hypertension.* 1991;18:565–574.
47. Lagerkranser M, Sollevi A, Irestedt L, Tidgren B, Andreen M. Renin release during controlled hypotension with sodium nitroprusside, nitroglycerin and adenosine: a comparative study in the dog. *Acta Anaesthesiol Scand.* 1985;29:45–49.
48. Bouma MG, van den Wildenberg FA, Buurman WA. Adenosine inhibits cytokine release and expression of adhesion molecules by activated human endothelial cells. *Am J Physiol.* 1996;270: C522–C529.
49. Dutka DP, Elborn JS, Delamere F, Shale DJ, Morris GK. Tumour necrosis factor alpha in severe congestive cardiac failure. *Br Heart J.* 1993;70:141–143.
50. Yang D, Zhang Y, Nguyen HG, Koupenova M, Chauhan AK, Makitalo M, Jones MR, Hilaire CS, Seldin DC, Toselli P, Lamperti E, Schreiber BM, Gavras H, Wagner DD, Ravid K. The A(2B) adenosine receptor protects against inflammation and excessive vascular adhesion. *J Clin Invest.* 2006;116:1913–1923.

CLINICAL PERSPECTIVE

Chronic heart failure is a major complication of myocardial infarction (MI) that substantially worsens its prognosis. Postinfarction remodeling includes progressive chamber dilatation, cardiac hypertrophy, and fibrosis. Fibrosis in the noninfarcted myocardium contributes to the pathogenesis of postinfarction cardiac dysfunction. Adenosine mediates cardioprotection against acute ischemia/reperfusion injury, mainly through adenosine A1, A2a, and A3 receptors. Adenosine also inhibits proliferation of cardiac fibroblasts and hypertrophy of cardiomyocytes, both of which may play crucial roles in cardiac remodeling. The present study demonstrated that long-term stimulation of adenosine receptors, begun 1 week after the onset of MI, improved hemodynamic and echocardiographic parameters. Long-term adenosine receptor stimulation reduced the collagen volume fraction and gene expression of the molecules associated with cardiac remodeling in noninfarcted myocardium. These improvements were blunted by the selective adenosine A2b antagonist. These data suggest that the long-term stimulation of adenosine A2b receptors begun after MI attenuates cardiac fibrosis in the noninfarcted regions and improves cardiac function. Drugs that stimulate adenosine A2b receptors or increase adenosine levels may be new candidates to attenuate post-MI cardiac remodeling.